Identification of Twelve Different Mineral Deficiencies in Hydroponically Grown Sunflower Plants on the Basis of Short Measurements of the Fluorescence and P700 Oxidation/Reduction Kinetics

Gert Schansker[1]*, Miho Ohnishi[2], Riu Furutani[2] and Chikahiro Miyake[2]*

[1]Heinz Walz GmbH, Effeltrich, Germany, [2]Department of Applied Biological Science, Graduate School for Agricultural Science, Kobe University, Kobe, Japan

The photosynthetic electron transport chain is mineral rich. Specific mineral deficiencies can modify the electron transport chain specifically. Here, it is shown that on the basis of 2 short Chl fluorescence and $P700^+$ measurements (approx. 1 s each), it is possible to discriminate between 10 out of 12 different mineral deficiencies: B, Ca, Cu, Fe, K, Mg, Mn, Mo, N, P, S, and Zn. B- and Mo-deficient plants require somewhat longer measurements to detect the feedback inhibition they induce. Eight out of twelve deficiencies mainly affect PS I and NIR measurements are, therefore, very important for this analysis. In Cu- and P-deficient plants, electron flow from the plastoquinone pool to PS I, is affected. In the case of Cu-deficiency due to the loss of plastocyanin and in the case of P-deficiency probably due to a fast and strong generation of Photosynthetic Control. For several Ca-, K-, and Zn-deficient plant species, higher levels of reactive oxygen species have been measured in the literature. Here, it is shown that this not only leads to a loss of Pm (maximum P700 redox change) reflecting a lower PS I content, but also to much faster $P700^+$ re-reduction kinetics during the I_2-P (~30–200 ms) fluorescence rise phase. The different mineral deficiencies affect the relation between the I_2-P and $P700^+$ kinetics in different ways and this is used to discuss the nature of the relationship between these two parameters.

Keywords: mineral deficiencies, P700-kinetics, polyphasic fluorescence rise, signatures, photosynthetic electron transport chain

INTRODUCTION

For optimal plant growth, a balanced diet of minerals is needed. If there is an insufficient supply of a particular mineral, this may lead to crop losses. It is possible to determine the mineral status of the soil by analyzing soil samples, however, for detection of mineral deficiencies, the plants growing on this soil can also be used. Since many of these mineral deficiencies

directly or indirectly affect the photosynthetic apparatus and its activity, non-invasive methods like chlorophyll (Chl) *a* fluorescence and near-infrared (NIR) absorption measurements have the potential to identify and detect the different mineral deficiencies.

Since the introduction of instruments for the measurement of Chl fluorescence and NIR kinetics (820 nm single channel measurements, P700 measurements derived from the difference between 830 and 870 nm, and deconvolution of PC, P700, and Fd signals on the basis of the measurement of 4 NIR wavelength pairs), it is possible to study the kinetics of photosystem (PS) II and PS I in detail. In a recent study, Ohnishi et al. (2021) characterized twelve mineral deficiencies on the basis of the kinetics of the operational quantum yield of PS II: Y(II), operational quantum yield of PS I: Y(I), yield of PS I donor side limitations: Y(ND), and yield of PS I acceptor side limitations: Y(NA) measured during 10 min of illumination, using a DUAL-PAM-100. This approach gives information on the impact of these 12 deficiencies on photosynthetic activity. For this study, also classical saturation pulses (300 ms high red-light intensity) and pulses for Pm-determinations (to determine the difference between all P700 oxidized and reduced) were applied to these plants. Here, we took these kinetic measurements and analyzed the polyphasic fluorescence rise and P700-kinetics during the first second of illumination focusing on lesions in the photosynthetic electron transport chain induced by these 12 deficiencies. Measurements of the polyphasic fluorescence rise and the simultaneously measured P700 kinetics give information on the reduction of the electron transport chain (Schansker et al., 2005). For the interpretation of the mineral deficiency data, we made use of the effect of the destruction of the manganese cluster (Tóth et al., 2007a), the effects of Mg and S-deficiency (Ceppi et al., 2012; Dinç et al., 2012), and the effects of salt stress (Çiçek et al., 2018) on the chlorophyll and 820 nm kinetics, considering as well, the relationship between the fluorescence kinetics and the plastoquinone (PQ) pool redox state (Tóth et al., 2007b).

To help the interpretation of the data, first an analysis of the literature was made. Ohnishi et al. (2021) worked with sunflower plants that were grown hydroponically. The following mineral deficiencies were induced: B-, Ca-, Cu-, Fe-, K-, Mg-, Mn-, Mo-, N-, P-, S-, and Zn-deficiency. What we want to show in this paper is, that short measurements of the Chl fluorescence and P700 kinetics of about 1 s contain enough information to identify specific signatures for each of these 12 mineral deficiencies.

Abbreviations: F_0, F_M, and F_V, minimum, maximum, and variable fluorescence; HIQ, high intensity quenching; O-I_1-I_2-P or OJIP, fluorescence rise between minimum and maximum fluorescence induced by high light intensity on a dark-to-light transition and defined by its intermediate steps; P700, PS I reaction center chlorophyll pair; PC, plastocyanin; Pm, maximum amplitude of the P700 signal (difference between all reduced and oxidized); Q_A and Q_B, primary and secondary quinone electron acceptors of PS II; Y(II) and Y(I), operational quantum yields of PS II and PS I, respectively; Y(ND) and Y(NA), quantum losses due to PS I donor and acceptor side limitations.

MATERIALS AND METHODS

Plant Material

Sunflower (*Helianthus annuus*) plants were grown in a growth chamber (14 h light at 27°C/10 h dark at 25°C; light intensity 300–400 μMol photons m^{-2} s^{-1}; relative humidity 50–60%). Seeds of sunflower were germinated in flowing tap water for 5 days in the growth chamber. Five-day-old seedlings were planted in pots filled with a hydroponic solution of half-strength Hoagland solution for 3 days. The plants were then transferred to full-strength Hoagland solution for 4 days. The composition of full-strength Hoagland solution is as follows: macronutrients [NH_4NO_3 (2 mM), KH_2PO_4 (0.8 mM), $CaCl_2$ (0.6 mM), and $MgSO_4$ (0.5 mM)]; micronutrients [H_3BO_4 (50 μM), $MnSO_4$ (9 μM), $ZnSO_4$ (0.7 μM), $CuSO_4$ (0.3 μM), Na_2MoO_4 (0.25 μM), and NaFeEDTA (45 μM)]. The pH of the nutrient solution was adjusted to 5.3–5.5, by adding 10 mM MES (2-morpholino ethanesulfonic acid) during cultivation. The plants were then transferred to the original Hoagland solution deprived of essential minerals (N, P, K, S, Ca, Zn, Mo, B, Fe, Mn, Cu, and Mg) for 1 week. Then, in the 1 week period after the 1 week of exposure to the treatment, the measurements of each sample were taken. The solutions were renewed once a week and always aerated with air. For all experiments, we measured the second leaves from the top of the plants.

Measurements of Fast PSI and PSII Kinetics

$P700^+$ absorbance and chlorophyll fluorescence were simultaneously measured using a Dual-PAM/F instrument (Walz, Effeltrich, Germany) with a closed leaf-type chamber (Bunkoukeiki Co., Ltd., Tokyo, Japan), in which expiratory air (assumed to be CO_2 saturated air) was let in and the temperature was set at 25 ± 0.1°C using a Peltier controller system (Bunkoukeiki Co., Ltd. Tokyo, Japan). Leaf disks (3.4 cm^2) from dark-adapted sunflowers were placed in the chamber.

Two types of kinetic measurements were analyzed here. Saturation pulse (SP) measurements consisting of 630 nm light pulses of 300 ms (16,000 μMol photons m^{-2} s^{-1}). For the determination of Pm, SP illumination was applied after 10 s of illumination with far-red light (720 nm).

WHAT DOES THE LITERATURE TELL US ABOUT THESE MINERAL DEFICIENCIES?

Cu-Deficiency

For the green alga *Chlamydomonas,* it was shown that in the case of Cu-deficiency, the copper containing plastocyanin is replaced by the iron-containing cytochrome c_6 as reviewed by Merchant et al. (2006). There are few studies on the physiological effects of copper deficiency on vascular plants, but also in plants plastocyanin would be a potential target. Ohnishi et al. (2021) indeed observed on the basis of DUAL-KLAS-NIR measurements, allowing the quantification of the PC signal,

that Cu-deficient plants have a much lower PC/P700 ratio. Another potential target is the Cu/Zn superoxide dismutase (SOD; Tainer et al., 1983; Bowler et al., 1992). Yamasaki et al. (2008) note that at low Cu-concentrations Cu/Zn-SOD is replaced by Fe-SOD in *Arabidopsis*.

P-Deficiency

Frydenvang et al. (2015) demonstrated for barley that P-deficiency made the I_2-step of O-I_1-I_2-P transient disappear. A similar effect was observed by Cetner et al. (2020) for radish plants. Frydenvang et al. (2015) could predict the severity of the treatment by quantifying this effect. In a subsequent paper (Carstensen et al., 2018), it was shown that P-deficiency effects were rapidly reversible. The authors showed as well that P-deficiency strongly reduced the orthophosphate content in the stroma. The authors concluded that P-deficiency leads to an inhibition of ATP-synthase. Looking at the electron transport chain, this could lead to a rapid build-up of Photosynthetic Control and, thus, slowdown of electron transfer from the PQ-pool to P700.

Mn-Deficiency

Husted et al. (2009) showed for Mn-deficient barley plants that their O-I_1-I_2-P transients behaved like transients of plants that had been exposed to a heat pulse in darkness (Srivastava et al., 1997; Tóth et al., 2005, 2007a) leading to a loss of their Mn-cluster. The authors write about genotypic differences between two barley varieties, but those differences look more like differences in the tolerance of the two varieties used to Mn-deficiency, with the variety Vanessa being considerably more tolerant than the variety Antonia. The differences in State Transitions observed by the authors may also be due to differences in the PS II electron donation capacity (depending on the severity of the deficiency) and associated differences in the PQ-pool redox state. In a follow-up paper, Birkelund Schmidt et al. (2013) showed that below a Mn-concentration of ~11 mg Mn kg^{-1} plant dry weight, the apparent F_V/F_M value correlated well with the Mn-content of the barley plants. In a third paper, the effects of the severity of the Mn-deficiency stress and recovery on the parameters of the quenching analysis (Φ_{PSII}, qP, and NPQ) were studied (Schmidt et al., 2016).

Fe- and S-Deficiencies

At the acceptor side of PS I, a high concentration of FeS-clusters is found of which three belong to PS I and ferredoxin also contains an FeS-cluster. Further, two FeS-clusters are found in the Rieske protein of the cytochrome b_6f complex and there is a non-heme iron in PS II located between Q_A and Q_B. Spiller and Terry (1980) studied the development of Fe-deficiency-related changes in "fairly" mature sugar beet leaves. Fe-deficiency developed within 10 days; this is considerably faster than the development of S-deficiency-related changes in another study on sugar beet leaves (Ceppi et al., 2012). This may also explain the fact that the Fe-deficiency-related changes observed here were considerably more severe than the S-deficiency-related changes. Stiller and Terry observed that, initially, P700 and

cyt f content decreased in parallel and was also paralleled by the loss of chlorophyll. The authors concluded that the plants lost electron transport chains, reflected by a reduction in the number of granal and stromal lamellae per chloroplast, but the photosynthetic unit size of the remaining electron transport chains was not affected. Only under severe stress conditions, the loss of P700 was considerably higher than the loss of cyt f and chlorophyll.

S-deficient sugar beet plants are also characterized by loss of the P700 + PC signal (Ceppi et al., 2012). There it was shown that for sugar beet leaves, the loss of the 820-nm signal correlated quite well with a decrease in the I_2-P amplitude.

Ca-, K-, and Zn-Deficiencies

Terry and Huston (1975) studied calcium deficiency in hydroponically grown sugar beet plants and found little effect of calcium deficiency on processes ranging from CO_2 assimilation to electron transport activities. Ridolfi et al. (1996) observed for Ca-deficient oak that it also caused a decrease of the Mg-content. In oak, Ca-deficiency had little effect on steady state fluorescence parameters, but Ca-deficient oak leaves showed more photorespiration. De Freitas et al. (2016) suggested a relationship between Ca-deficiency, gibberellic acid, and ROS scavenging capacity. Although no solid experimental proof for this suggestion was provided, it fits best with the experimental observations obtained for the sunflower plants studied here.

Also, K-deficiency has been associated with increased ROS production. Cakmak (2005) noted in a review that evidence is accumulating that improvement of the potassium nutritional status of plants can greatly lower the ROS production. Though many factors related to K-deficiency have been described in the literature the exact mechanism by which K-deficiency negatively affects photosynthesis remains unclear.

As noted above, one of the superoxide dismutases is a Cu/Zn superoxide dismutase. This enzyme may be a target for Zn-deficiency. And this could then lead to higher levels of ROS, damage to the acceptor side of PS I and a loss of Pm-amplitude.

Based on the literature Mg- and N-deficiency also have been associated with higher levels of ROS, but these deficiencies also induce additional deficiency-related changes and will, therefore, be discussed separately (see below).

Mg-Deficiency

An early response of plants to Mg-deficiency is a strong accumulation of sugar and starch (Fischer and Bremer, 1993; Hermans et al., 2005; Cakmak and Kirkby, 2008). Mg-deficiency also leads to a light intensity-dependent loss of chlorophyll (Cakmak and Kirkby, 2008; Peng et al., 2019), which does not lead to a change in the chl a/b ratio, nor does it affect the functionality of the remaining electron transport chains (Terry and Ulrich, 1974; Dinç et al., 2012). Another symptom of Mg-deficiency is the destacking of thylakoid membranes as, for example, observed in maize (Hall et al., 1972). For sugar beet leaves, it was suggested that destacking and an associated increase in spillover could be responsible for some

of the observed phenomena (Dinç et al., 2012). The literature further suggests that Mg-deficiency in a late stage increases ROS levels and may, therefore, cause damage to the PS I acceptor side with an associated loss of the Pm-amplitude (Cai et al., 2019; Hauer-Jákli and Tränkner, 2019; Peng et al., 2019).

B- and Mo-Deficiencies

Boron deficiency leads to an accumulation of sugar in olive leaves (Liakopoulos et al., 2005). For *Citrus sinensis,* both increased leaf levels of starch and hexoses (Han et al., 2008) and an accumulation of phenolics and a decreased nitrate reductase activity have been described (Lu et al., 2014). For *Brassica rapa* leaves, starch accumulation was reported (Hajiboland and Farhanghi, 2010). Feedback inhibition of photosynthesis due to the accumulation of synthates has been suggested (e.g., Dell and Huang, 1997).

With respect to Mo-deficiency, there are quite a few articles that describe in detail all enzymes that contain Mo as a cofactor. However, the impact on the activity of the electron transport chain is rarely described. Molybdenum is a cofactor of nitrate reductase. Mahler (1982) writes that Mo-deficient non-legume plants cannot make use of nitrate taken up by the roots. As a consequence, Mo-deficiency induces N-deficiency and in the field, it is difficult to discriminate between Mo- and N-deficiency. Ide et al. (2011) analyzed the metabolic profile of Mo-deficient plants and noted a decrease in amino acids and an increase in sugars and sugar phosphates related to an increase in the carbon to nitrogen ratio. The increased sugar levels could lead to feedback inhibition.
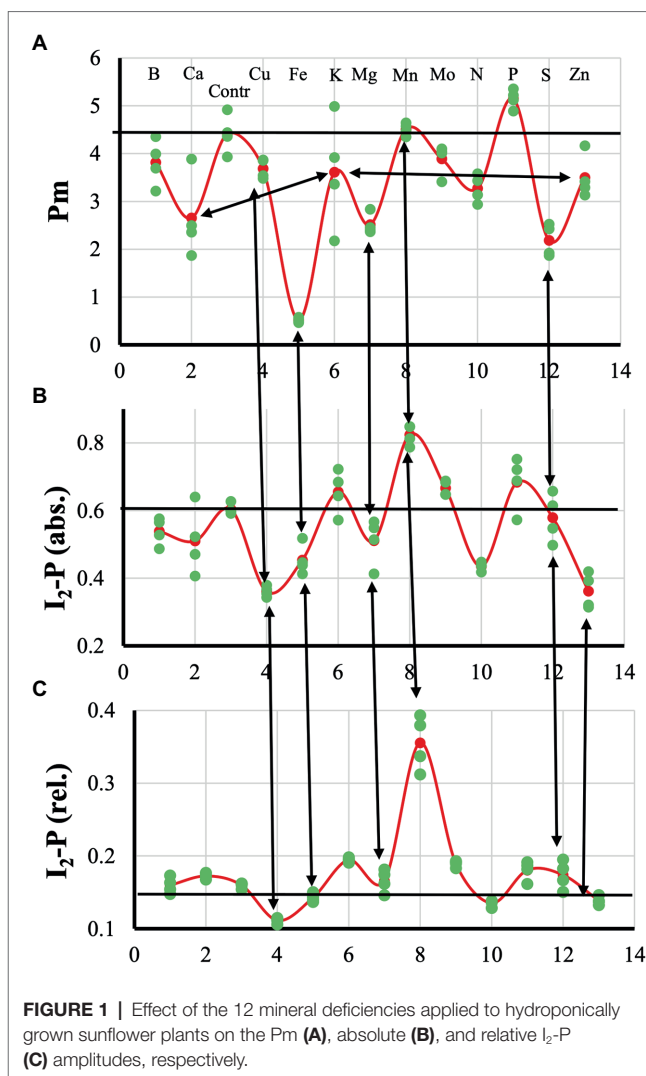
N-Deficiency

Evans and Terashima (1988) concluded that N-deficiency had no effect on photosynthetic activities when calculated on a chlorophyll basis. Oxidative stress has been described though. Shao et al. (2020) observed for rice that N-deficiency leads to increased H_2O_2 production and lipid peroxidation. Nguyen et al. (2003) found for *Melaleuca* and *Eucalyptus* species grown under N-deficient conditions an accumulation of starch and sugars in different parts of these plants, also in the leaves, suggesting that N-deficiency may lead to feedback inhibition.

EXPERIMENTAL OBSERVATIONS DERIVED FROM THE DATASET

Figure 1 gives an overview of the effects of the different mineral deficiencies on the Pm (**Figure 1A**), the absolute (**Figure 1B**) and relative I_2-P amplitude (**Figure 1C**). In **Supplementary Figure 1**, all averages were normalized to the control values. These data will be discussed in the context of the different deficiencies.
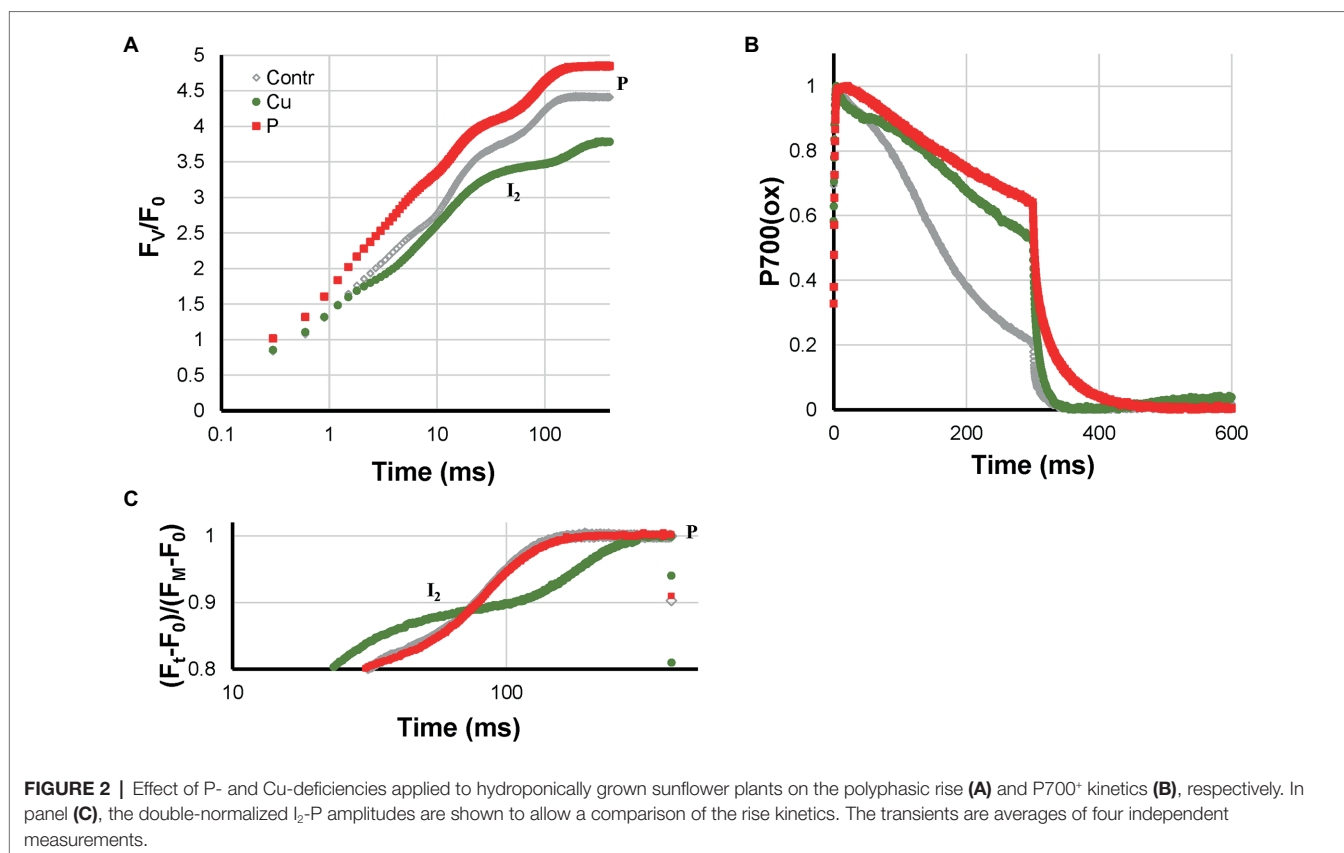
Cu- and P-deficiency both affected the electron flow from the PQ-pool to P700. In both cases, the re-reduction of $P700^+$ during the I_2-P phase was very slow. At the P-level, in both cases, around 60% of P700 remained in the oxidized state (**Figure 2B**). Differences between the two are that

FIGURE 1 | Effect of the 12 mineral deficiencies applied to hydroponically grown sunflower plants on the Pm **(A)**, absolute **(B)**, and relative I_2-P **(C)** amplitudes, respectively.

P-deficient plants had an F_V/F_0 that was considerably higher than the Control and no HIQ (high intensity quenching, lowering of the fluorescence intensity due to the formation of fluorescence quenching carotenoid radicals in the light; Schreiber et al., 2019); Cu-deficient plants had an F_V/F_0 value that was considerably smaller than the Control and a little bit of HIQ (in **Figures 3, 4** the position of the more prominent HIQ is indicated with an arrow). Further, the I_2-P kinetics of P-deficient and Control plants were very similar, whereas, in the case of Cu-deficiency, slower kinetics and a considerable lag-phase were observed (**Figures 2A,C**). In addition, the $P700^+$ re-reduction kinetics were more complex in the case of Cu-deficient plants and the effect of the deficiency on the fraction loss of I_2-P (abs.) and I_2-P (rel.) was stronger than the fraction Pm loss (see **Supplementary Figure 1**).

Mn-deficiency was expected to lead to a gradual loss of Mn-clusters of the PS II reaction centers. It was, therefore, expected that Mn-deficient plants behaved like heat-pulse-treated plants, which have a very limited PS II electron donation capacity. This was indeed observed as: slow reduction kinetics
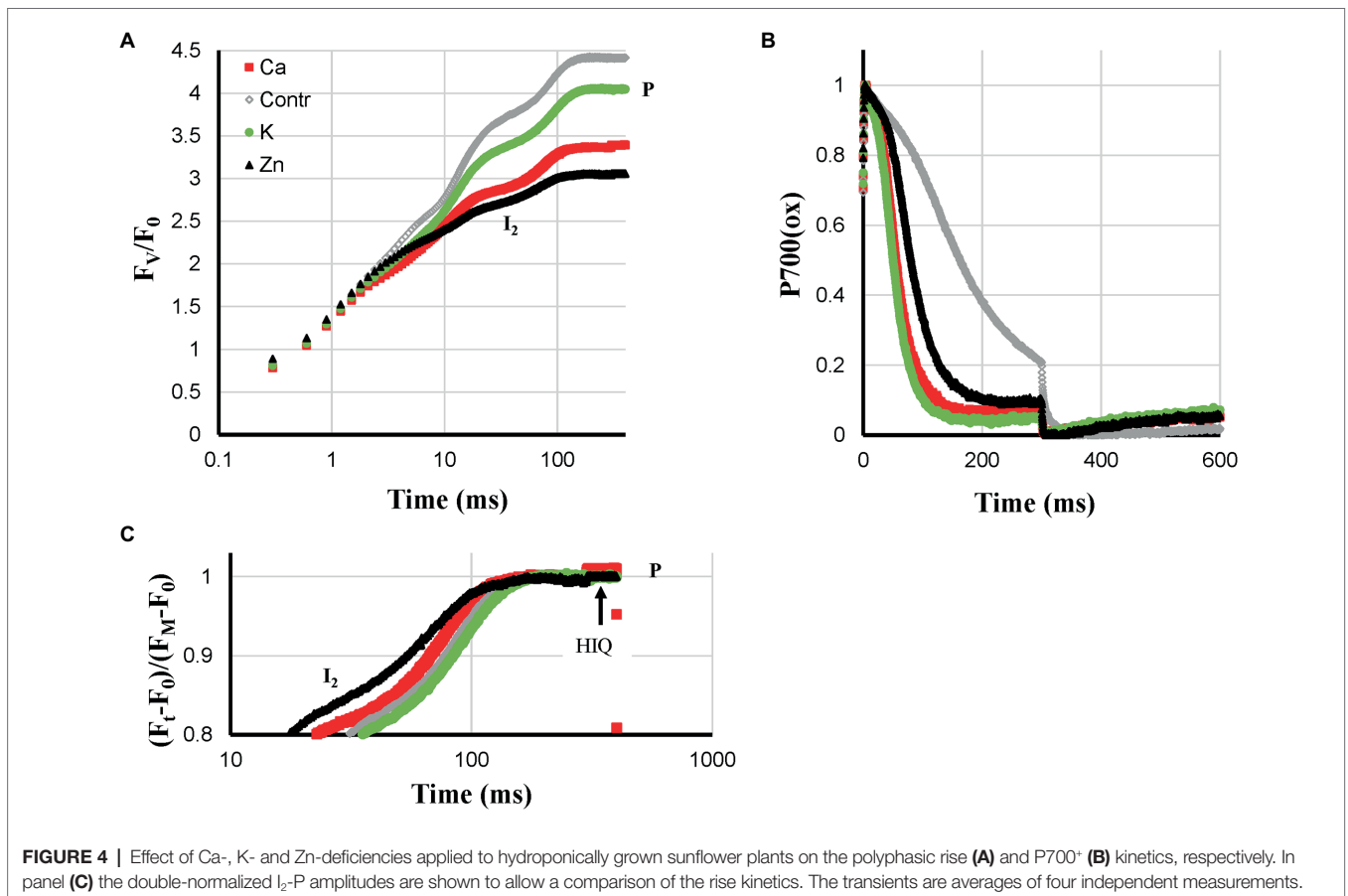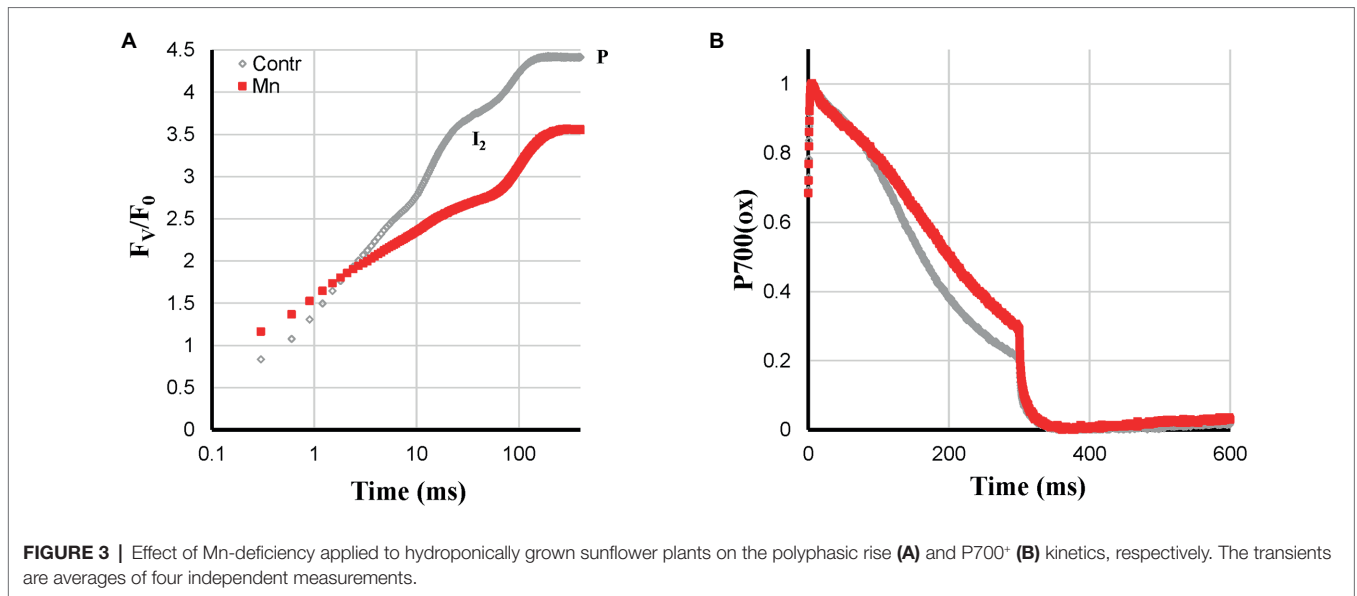
FIGURE 2 | Effect of P- and Cu-deficiencies applied to hydroponically grown sunflower plants on the polyphasic rise **(A)** and P700+ kinetics **(B)**, respectively. In panel **(C)**, the double-normalized I_2-P amplitudes are shown to allow a comparison of the rise kinetics. The transients are averages of four independent measurements.

of the electron transport chain, by far the largest I_2-P amplitude and an associated quite strong reduction of F_V/F_0 (**Figure 3A**). The P700+ re-reduction kinetics on the other hand were not too different. The re-reduction of the Mn-deficient leaves was less complete, which may be related to the lower electron donation capacity of PS II (**Figure 3B**). Compared to the Mn-deficiency-related changes of the barley variety Antonia described by Husted et al. (2009), the effect of the treatment on these sunflower plants was still rather mild.

For Ca-, K-, and Zn-deficiencies, higher ROS levels have been described and these three deficiencies led to a loss of Pm: Ca > K > Zn. Ca- and K-deficient plants both showed very fast P700+ re-reduction kinetics during the I_2-P phase. These kinetics were somewhat slower in Zn-deficient plants but still much faster than in the Control plants (**Figure 4B**). HIQ was present but not very strong in Ca-deficient plants, very small in Zn-deficient plants, and absent in K-deficient plants. Further, Ca- and Zn-deficient plants showed quite low F_V/F_0 values of approx. 3.35 and 3.05, respectively, compared with approx. 4.05 for K-deficient plants (**Figures 4A,C**). In **Figure 3C**, the I_2-P rise kinetics of fluorescence transients double-normalized between O and P are shown, indicating that Zn-deficient plants had the fastest rise time followed by Ca-deficient plants. The rise times observed for the Control and K-deficient plants are similar.

Fe- and S-deficient plants were expected to synthesize fewer FeS-clusters and as a consequence have a lower PS I content. These two deficiencies showed the strongest loss of Pm; however,

the development of deficiency-related changes was considerably faster and stronger in Fe-deficient plants than in S-deficient plants. Fe-deficiency led to faster P700+ re-reduction kinetics during the I_2-P rise, a symptom that was not pronounced in the S-deficient leaves (**Figure 5B**). The fast P700+ re-reduction kinetics described for Ca-, K-, and Zn-deficiencies described above may also be explained by a ROS-induced damage to the FeS-clusters of the PS I acceptor side. Higher ROS levels due to a loss of the Fe-SOD could be an explanation for the fast P700+ re-reduction kinetics observed for the Fe-deficient plants that is missing in the case of S-deficient plants. Despite the difference in Pm-amplitude (88% loss in Fe-deficient leaves compared with 50% loss in S-deficient leaves), the induction curves of Fe- and S-deficient plants were quite similar. Both curves showed a partially reduced PQ-pool (Tóth et al., 2007b), an F_V/F_0-value of about 4 and HIQ (**Figure 5A**). The partially reduced PQ-pool in darkness was also observed under quite severe S-deficient conditions in sugar beet (Dinç et al., 2012). This was not observed for Ca-, K-, N-, and Zn-deficient plants, where the smaller Pm may be due to ROS-induced destruction of the PS I acceptor side.

Based on the literature, Mo- and B-deficiency could lead to feedback inhibition (see above). Mo- and B-deficiency had no effect on Pm and showed only a small decrease of F_V/F_0 (**Figure 6A**). Mo-deficient plants showed a strong reduction of the PQ-pool in darkness with an associated broad I_2-step (Tóth et al., 2007b). Further, Mo-deficient plants showed an
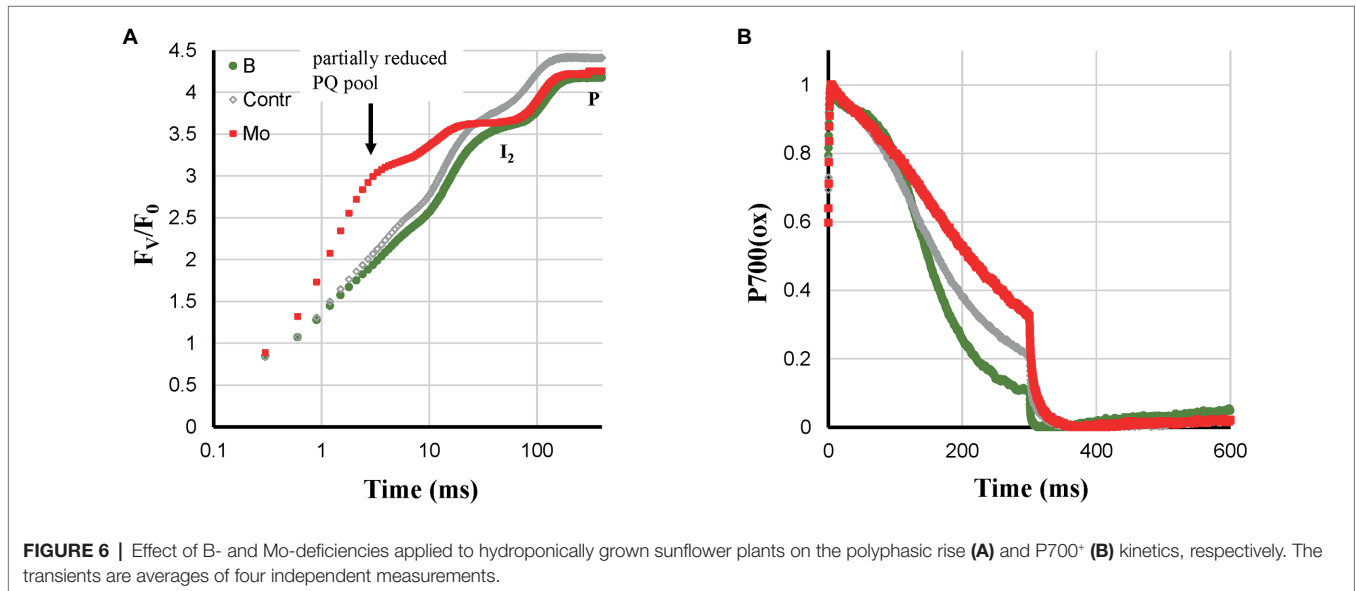
FIGURE 3 | Effect of Mn-deficiency applied to hydroponically grown sunflower plants on the polyphasic rise **(A)** and P700+ **(B)** kinetics, respectively. The transients are averages of four independent measurements.

FIGURE 4 | Effect of Ca-, K- and Zn-deficiencies applied to hydroponically grown sunflower plants on the polyphasic rise **(A)** and P700+ **(B)** kinetics, respectively. In panel **(C)** the double-normalized I$_2$-P amplitudes are shown to allow a comparison of the rise kinetics. The transients are averages of four independent measurements.

incomplete re-reduction of P700+ (**Figure 6B**) and HIQ. B-deficient plants had more sigmoidal P700+ re-reduction kinetics than the Control (**Figure 6B**) and showed no HIQ. However, these two types of plants are better defined by an almost non-existent P700-donor side limitation Y(ND)

and a high PS I acceptor side limitation Y(NA) during most of a 10 min induction period (Ohnishi et al., 2021).

N-deficient plants showed a mix of deficiency-related changes. The quite strong Pm loss was also observed like for Ca-, K-, and Zn-deficiencies (**Figure 1C**). However, the associated fast
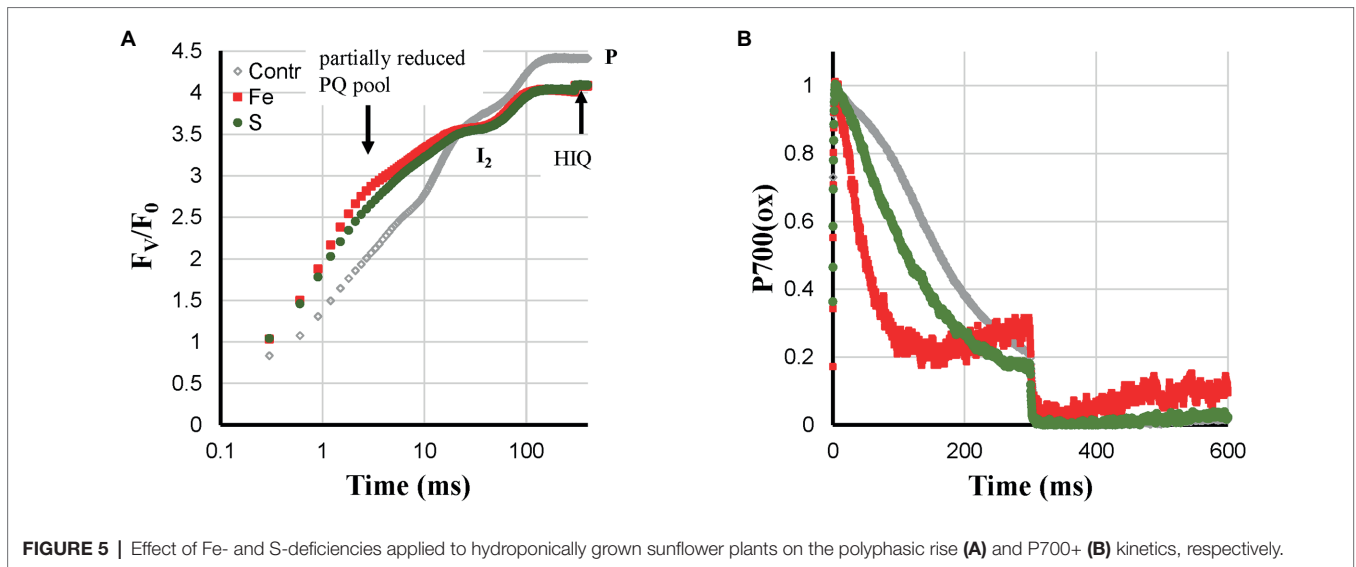
FIGURE 5 | Effect of Fe- and S-deficiencies applied to hydroponically grown sunflower plants on the polyphasic rise **(A)** and P700+ **(B)** kinetics, respectively.

FIGURE 6 | Effect of B- and Mo-deficiencies applied to hydroponically grown sunflower plants on the polyphasic rise **(A)** and P700$^+$ **(B)** kinetics, respectively. The transients are averages of four independent measurements.

P700-re-reduction was missing (**Figure 7B**), and this could be due to feedback inhibition. The N-deficient plants did show HIQ (**Figure 7A**).

The symptoms observed for Mg-deficient plants were a fractional Pm loss that was stronger than the I$_2$-P (abs.) loss and there was nearly no effect on I$_2$-P (rel.) compared to the Control, see **Supplementary Figure 1**. Increased ROS levels have also been described in the literature for Mg-deficiency, which could be responsible for the decrease of Pm. The absence of faster P700$^+$ re-reduction kinetics (**Figure 7B**) could then be due to a counteracting effect of destacking induced by Mg-deficiency causing a mixed state as observed for N-deficiency.
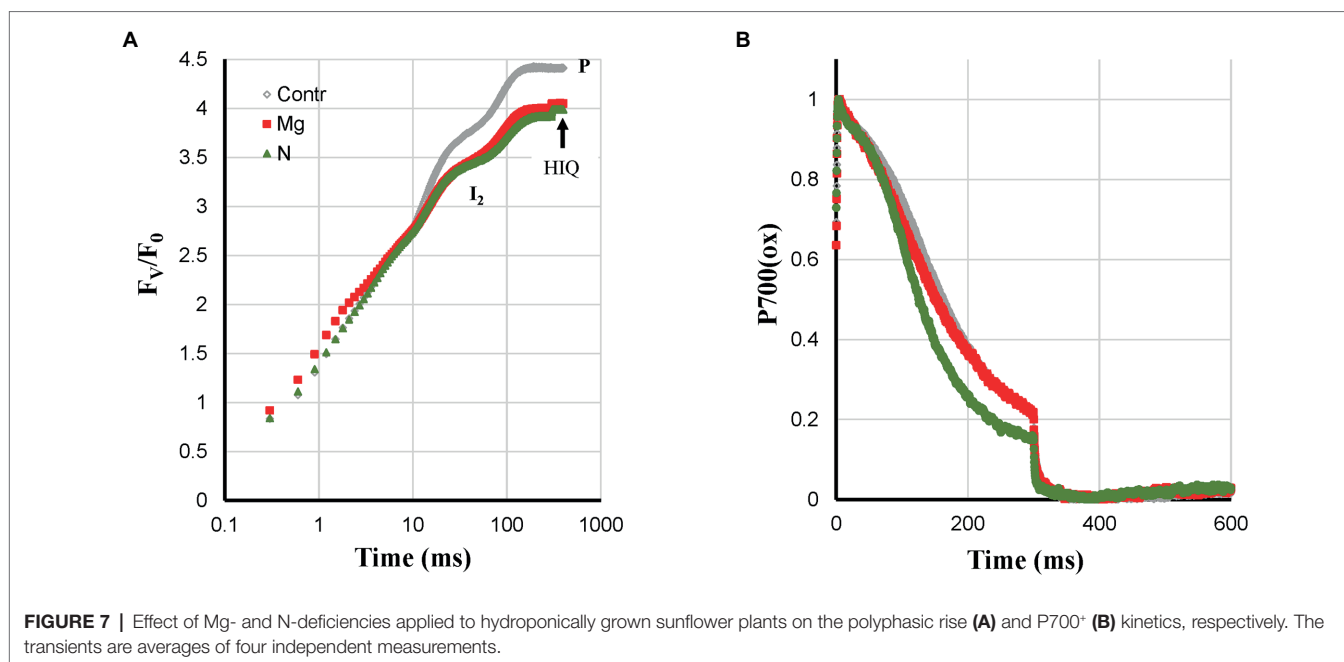
For a general application of this data, more information on the development of the deficiency-related changes in each case would be needed, but the data show that it is possible to discriminate between the twelve deficiencies that were induced in these sunflower plants.

DISCUSSION

Diagnosis of Mineral Deficiencies

As shown above, for the present dataset on 12 mineral deficiencies, there is enough kinetic information to separate all 12 of them. Mn-deficiency stands alone. Only Mn can be used for a functional Mn-cluster. The other 11 deficiencies can be assigned to 4 different classes, with N-deficiency possibly belonging to two different classes: 1. P- and Cu-deficiency affecting the electron flow between the PQ-pool and P700; 2. Ca-, K-, and

FIGURE 7 | Effect of Mg- and N-deficiencies applied to hydroponically grown sunflower plants on the polyphasic rise **(A)** and P700+ **(B)** kinetics, respectively. The transients are averages of four independent measurements.

Zn- (and N-) deficiency associated with damage to the PS I acceptor side and fast P700+ re-reduction kinetics; 3. Fe- and S-deficiency affecting the synthesis of FeS-clusters; and 4. Mo- and B- (and N-) deficiency leading to feedback inhibition. The Mg- and N-deficiencies are treated in a separate figure (**Figure 7**) representing mixed states; they show a loss of Pm, but the P700+ re-reduction kinetics are not faster than in the control. For these four classes, the challenge is to separate in each case the class-members. For each deficiency, there is one time point available. It is, therefore, not possible to judge at what point during the development of the different deficiencies it is possible to separate them. It would seem likely that during early stages of the mineral deficiency the effects will be too small or too aspecific for a precise diagnosis. However, more extensive research would be needed to determine this.

Biological Variability Between Plant Species: Electron Flow From the PQ-Pool to P700

Although the data analyzed here, confirm observations made earlier for other plant species, the kinetic properties of sunflower leaves seem to differ from, for example, sugar beet leaves. In sugar beet leaves, a reasonable correlation between I_2-P and the P700+PC signal was observed (Ceppi et al., 2012). Here, a P700 loss did translate itself into a proportionally smaller I_2-P amplitude, but with a considerable offset (see **Figure 8** and "Correlation Between I_2-P and Pm Amplitudes"). Possibly, the limitation posed by the cyt b_6f complex in sunflower is considerably stronger than in sugar beet. This was supported by observations made on P-deficient plants. In the literature, it has been described for P-deficient barley and radish plants that this led to a loss of the I_2-step (Frydenvang et al., 2015; Carstensen et al., 2018; Cetner et al., 2020). In sunflower, this was not observed. However, in the case of Fe- and S-deficient plants, it should also be considered

that the Rieske protein of cyt b_6f of sunflower could be more sensitive to these deficiencies than that of sugar beet.

Interpretation of the Polyphasic Fluorescence Rise

Fluorescence induction curves: O-I_1-I_2-P or O-J-I-P are kinetically complex. And there is still no consensus on the role of the underlying processes. The redox state of Q_A is the dominant factor, but there are several other factors that may play a larger or smaller role. E.g., transient accumulation of P680+, especially when very high pulse-light-intensities are used (higher than 5,000 µMol photons m^{-2} s^{-1}). Morin (1964) and Delosme (1967) discriminated between a photochemical phase reflecting the reduction of Q_A and a thermal phase reflecting another process sensitive to the temperature. With modern instruments, it is possible to quantify the photochemical phase very precisely by inducing the O-I_1 rise by strong light, giving a single turnover flash after 1 ms to make sure that all Q_A is reduced. Although people have speculated about variable PS I fluorescence for many years there was no clear experimental evidence for its existence in leaves. Tóth et al. (2005) showed for several plant species that well dark-adapted leaves, subsequently passively infiltrated with DCMU, had F_M-values that were independent of the redox state of PS I. Nearly identical F_M-values were observed in either the presence or absence of DCMU. Two recent publications treat this topic experimentally in intact organisms (Pfündel, 2021; Schreiber and Klughammer, 2021). By measuring at wavelengths shorter than 710 nm and longer than 700 nm, respectively, a comparison could be made between induction curves reflecting mainly PS II emission and curves reflecting both PS II and PS I emission. Schreiber and Klughammer (2021) could clearly show a role of variable PS I fluorescence in green algae and cyanobacteria. In light green young *Hedera* leaves, they also detected variable
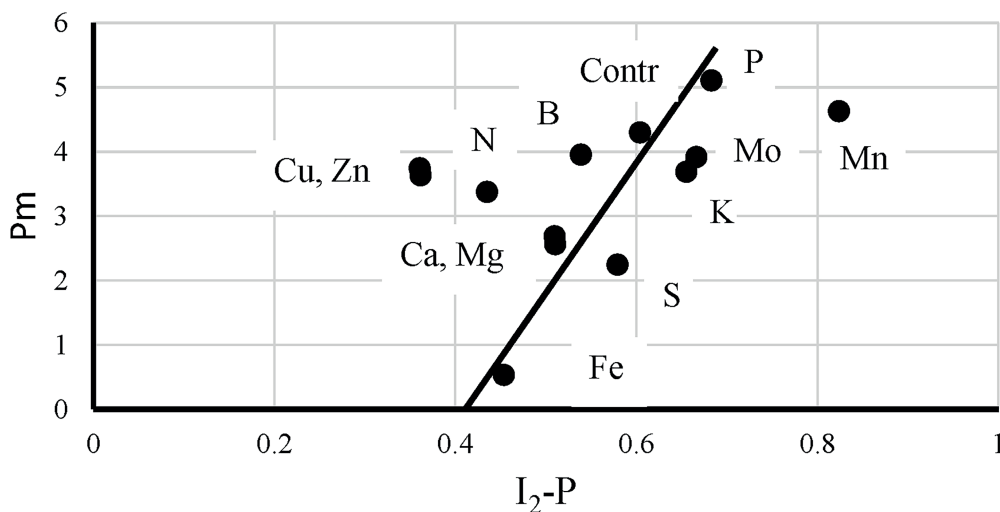
FIGURE 8 | The relationship between the P700$^+$(I$_2$-P) and I$_2$-P kinetics measured on leaves of control plants and of plants exposed to 12 mineral deficiencies. The points are averages of four independent measurements.
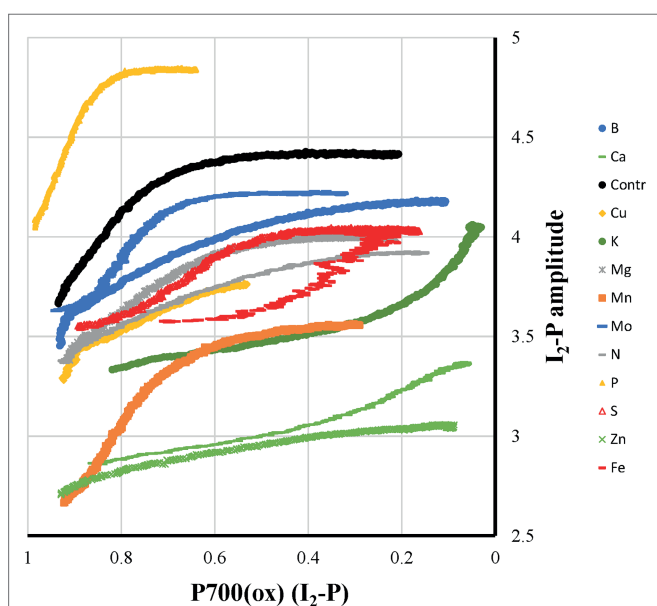
FIGURE 9 | Relationship between Pm and I$_2$-P amplitude for plants exposed to 12 mineral deficiencies. The colors reflect the different classes: yellow, electron transfer between cyt b_6f and P700 affected; green, PS I acceptor side damage; red, FeS-cluster synthesis affected; blue, feedback inhibition; and gray, mixed states. Further, Mn-deficiency is orange, and the Control is black. The data represent averages of four independent measurements.

PS I fluorescence, whereas Pfündel (2021) working with dark, mature *Prunus laurocerasus* leaves concluded that there was no variable PS I fluorescence. Analytically, a difference between both studies was that Schreiber and Klughammer (2021) normalized their data to the O-I$_1$ amplitude, whereas Pfündel (2021) normalized his data on the variable fluorescence. However, could it be that biological variability between plant species as

illustrated in the previous paragraph is a more important reason for this discrepancy? The sunflower data discussed here compared to observations made on barley and sugar beet could support effects of such biological variability.

Do Sunflower Plants Show Variable PS I Fluorescence?

If variable PS I fluorescence exists in sunflower plants, we would expect it to develop during the I$_2$-P phase. Only during this kinetic phase, a reduction of both the donor and acceptor side of PS II occurs, creating a PS II like state. If there is variable PS I fluorescence you would expect at the end of the PS I reduction phase a more or less linear correlation between the redox state of P700 and the fluorescence rise. In **Figure 9**, these two parameters are shown as a function of each other. For most of the mineral deficiencies, the relationship consists of a fast fluorescence increase in the beginning, where most P700 is still in the oxidized state, followed by no or a slow fluorescence increase while most of the P700$^+$ is re-reduced. The casual observer may think that K-, Ca-, and Fe-deficiencies may form an exception. However, the upward curve of the relationship on going to full P700$^+$ reduction is due to faster P700$^+$ reduction kinetics without changes in the kinetics of the I$_2$-P rise. In other words, this would point more toward the absence of a relationship between the two parameters. At the other extreme, we have P-deficient plants, where at 20% reduced P700, P is almost reached. Comparing the double-normalized I$_2$-P kinetics of Control and P-deficient plants, they are essentially identical (**Figure 2C**). This strongly suggests that the I$_2$-P rise is determined in sunflower by kinetic factors not directly related to the PS I and P700 redox state. This would support, at least for sunflower plants, the conclusions of Pfündel (2021).

Correlation Between I_2-P and Pm-Amplitudes

Ceppi et al. (2012) showed for S-deficiency that the 820 nm signal correlated with the I_2-P amplitude, both relative and absolute, in sugar beet leaves. As shown by Çiçek et al. (2018) for chickpea, this correlation breaks down if electron transfer between the cyt b_6f complex and P700 is inhibited by salt stress. In **Figure 8**, this relationship is checked for the sunflowers used in this study. Instead of the maximum P700 + PC signal, the Pm is plotted here as a function of I_2-P (abs.). A trendline was drawn through the core set of points. The plot has two clear outliers. In Mn-deficient plants, PS II generates too few electrons to allow a saturation of the I_2-step. As a consequence, the I_2-P amplitude is proportionally larger than the I_2-P amplitude of any of the other deficiencies (e.g., **Supplementary Figure 1**). On the other side, Cu is a clear outlier. The loss of PC has a kinetic effect on the I_2-P amplitude, making it smaller. Zn is also an outlier, but in that case, it probably has to do with the loss of variable fluorescence (see **Figure 4A**). Finally, N also lies outside the trendline. As **Figure 7A** shows, N-deficient plants, like Cu-deficient plants, have relatively slow I_2-P rise kinetics, although no clear reason for this feature can be provided. The trendline suggests that the "Pm is 0" line intersects the I_2-P axis around 0.4. This could mean that not the whole I_2-P phase is sensitive to the presence of PS I, or, which is maybe more likely, that the inflection point that is considered the I_2 step overestimates the I_2-P amplitude, because it still contains a considerable contribution of the I_1-I_2 phase. Or a mix of both. Ignoring this offset, though, there seems to be a rough correlation between I_2-P and Pm in sunflower as well. However, comparing the sugar beet and sunflower data clearly illustrates the kinetic variability between plant species.

Another example of an experiment that was interpreted to show that there is no correlation between I_2-P phase and PS I was published by Zivcak et al. (2015). These authors applied a series of strong 300 ms pulses spaced 10 s apart and assumed that their treatment predominantly inactivated PS I. The authors wrote that a decrease of F_V/F_M from 0.78 to 0.72 equated an 8% decrease. However, as a simple calculation shows, at the same time, this 8% F_V/F_M decrease equates an almost 28% decrease in F_V. As was shown in several studies, O_2-evolution extrapolates to zero around an F_V/F_M of 0.4–0.44 (Van Wijk and Krause, 1991; Schansker and Van Rensen, 1999) and 0.06/0.38 would already equate a decrease of 16%. If we would assume that the maximum quantum yield of the control would equate the literature value of 0.84, the decrease would further increase to 27%. In other words, the damage done by the treatment to PS II was in this case considerably stronger than the authors assumed. As a consequence, the fact that they did not observe an effect of their treatment on the relative I_2-P amplitude provides little experimental basis for their thesis that PS I activity did not affect the fluorescence rise. A chilling experiment could in this respect have provided the authors with a method to damage PS I more specifically.

P-Deficiency, Inhibition of ATP-Synthase, and Photosynthetic Control

Carstensen et al. (2018) showed for P-deficient barley plants a drop in the stromal P-concentrations and suggested on that basis that P-deficiency led to inhibition of ATP-synthase. On the basis of the measurements discussed here, this effect cannot be measured directly. However, low ATP-synthase activity will slow down the export of protons from the lumen to the stroma and is, therefore, expected to lead to an accelerated acidification of the lumen, which in turn will accelerate the slowdown of the re-oxidation of plastoquinol by the cyt b_6f complex. In other words, it will speed up the generation of Photosynthetic Control. This interpretation is confirmed by the slow P700$^+$ re-reduction kinetics observed in **Figure 2B**. The fact that under these conditions, P is reached while still more than 60% of P700 is in the oxidized state (**Figure 9**) has important implications for our understanding of Chl a fluorescence measurements. Together with the PC-loss occurring in Cu-deficient plants (Ohnishi et al., 2021), this offers experimenters two very interesting model systems for the study of electron flow from the PQ-pool to PS I as well as processes like the xanthophyll cycle and NPQ-formation that are regulated by the lumen pH.

Faster P700$^+$ Re-Reduction in Ca-, K-, and Zn-Deficient Plants

Another new experimental observation is formed by the much faster P700$^+$ re-reduction kinetics during the I_2-P phase (**Figure 4**) observed for deficiencies that according to the literature cause increased ROS levels (Tainer et al., 1983; Bowler et al., 1992; Cakmak, 2005; De Freitas et al., 2016). These kinetics were associated with a Pm loss but not accompanied by faster I_2-P rise kinetics. For the S-deficient plants, a stronger Pm loss was observed (**Figure 5B**) but there the P700$^+$ re-reduction kinetics were considerably slower (**Figure 5B**). It suggests that the effect is not determined by PS I content. If the deficiency-induced ROS would lead to damage and inactivation of the FeS-clusters on the acceptor side of PS I it would strongly reduce the pool of electron acceptors available on the acceptor side of PS and this could explain the observed faster kinetics. That would mean that the faster kinetics are not a reflection of a loss of PS I but would then reflect the presence of PS I reaction centers with a damaged acceptor side. The data on N-, Mg-, and Fe-deficient plant suggest though that this ROS-induced effect may remain partially hidden if the deficiency causes other lesions: feedback inhibition in the case of N-deficiency, destacking in the case of Mg-deficiency, and a lower PS I synthesis in the case of Fe-deficiency.

Signatures

An important goal in quite a few fluorescence studies is to define stress effects on the fluorescence kinetics that allow an unambiguous identification of different stresses. We had the same ambition here. Below a signature is defined for the twelve different deficiencies.

Mn-Deficiency

Slower fluorescence rise, large I_2-P amplitude (lower F_V/F_0 ratio), and no effect on the Pm amplitude.

P-Deficiency

Like Cu-deficiency, slow and very incomplete P700$^+$ re-reduction kinetics during the I$_2$-P phase. Only deficiency that leads to higher F$_V$/F$_0$ ratio than in Control plants and I$_2$-P rise kinetics that are nearly the same as in Control plants.

Cu-Deficiency

Like P-deficiency, slow and very incomplete P700$^+$ re-reduction kinetics during the I$_2$-P phase, however, these kinetics were more complex. Lower F$_V$/F$_0$ ratio than in Control plants and slower I$_2$-P rise kinetics accompanied by a lag-phase.

S-Deficiency

Strong Pm loss (50% of Control), partially reduced PQ-pool in darkness, relatively strong HIQ signal, only slightly faster P700$^+$ re-reduction kinetics during the I$_2$-P phase.

Fe-Deficiency

Strong Pm loss (12% of Control), partially reduced PQ-pool in darkness, relatively strong HIQ signal, in contrast to S-deficient plants fast P700$^+$ re-reduction kinetics during the I$_2$-P phase.

Ca-Deficiency

Fast P700$^+$ re-reduction kinetics during the I$_2$-P phase, no PQ-pool reduction in darkness, small HIQ signal, Pm loss, but no effect on the relative I$_2$-P amplitude, relative small F$_V$/F$_0$ ratio (3.35).

K-Deficiency

Fast P700$^+$ re-reduction kinetics during the I$_2$-P phase, no PQ-pool reduction in darkness, no HIQ signal, Pm loss, but no effect on the relative I$_2$-P amplitude, relative large F$_V$/F$_0$ ratio (4.05).

Zn-Deficiency

Slightly slower P700$^+$ re-reduction kinetics during the I$_2$-P phase than observed for Ca- and K-deficient plants, no PQ-pool reduction in darkness, nearly no HIQ signal, Pm loss, but nearly no effect on the relative I$_2$-P amplitude, small F$_V$/F$_0$ ratio (3.05).

Mg-Deficiency

No effect on the P700$^+$ re-reduction kinetics during the I$_2$-P phase, no PQ-pool reduction in darkness, small HIQ signal, fraction Pm loss > fraction I$_2$-P (abs.) loss, no effect I$_2$-P (rel.).

B-Deficiency

More sigmoidal P700$^+$ re-reduction kinetics during the I$_2$-P phase than in Control plants, no PQ-pool reduction in darkness, no HIQ signal, high Y(NA), and little Y(ND) during most of 10 min of actinic illumination.

Mo-Deficiency

Incomplete re-reduction of P700$^+$ at P, partial reduction of the PQ-pool, small HIQ signal, no Pm loss and no effect on I$_2$-P amplitude, high Y(NA), and little Y(ND) during most of 10 min of actinic illumination.

N-Deficiency

Only somewhat faster P700$^+$ re-reduction kinetics during the I$_2$-P phase than in Control plants, no PQ-pool reduction in darkness, relatively strong HIQ signal, Pm loss comparable to K- and Zn-deficiency. Fractional Pm, I$_2$-P (abs.) and I$_2$-P (rel.) loss were similar.

DATA AVAILABILITY STATEMENT

The raw data supporting the conclusions of this article will be made available by the authors, without undue reservation.

AUTHOR CONTRIBUTIONS

Reading the paper of Ohnishi et al. (2021) published in antioxidants, GS asked the authors if they were willing to share the fast kinetic data, they measured but did not use in their paper. On the basis of these measurements, GS made an analysis of the shared data and wrote the paper. With respect to the experimental research used for this analysis, CM conceived the research plan and was involved in the original analysis of the data. MO did most of the experiments. RF designed the experiments and was involved in the original analysis of the data. All authors contributed to the article and approved the submitted version.

FUNDING

ACKNOWLEDGMENTS

SUPPLEMENTARY MATERIAL

The Supplementary Material for this article can be found online at: https://www.frontiersin.org/articles/10.3389/fpls.2022.894607/full#supplementary-material

SUPPLEMENTARY FIGURE 1 | The average values from **Figure 1** were taken, normalized to the Control values, and shown in a single figure to allow an easy comparison of relative changes in the parameters Pm, I$_2$-P (abs.), and I$_2$-P (rel.).

REFERENCES

Birkelund Schmidt, S., Pedas, P., Holst Laursen, K., Schjoerring, J. K., and Husted, S. (2013). Latent manganese deficiency in barley can be diagnosed and remediated on the basis of chlorophyll *a* fluorescence measurements. *Plant Soil* 372, 417–429. doi: 10.1007/s11104-013-1702-4

Bowler, C., Van Montagu, M., and Inzé, D. (1992). Superoxide dismutase and stress tolerance. *Annu. Rev. Plant Physiol. Plant Mol. Biol.* 43, 83–116. doi: 10.1146/annurev.pp.43.060192.000503

Cai, Y.-T., Zhang, H., Qi, Y.-P., Ye, X., Huang, Z.-R., Guo, J.-X., et al. (2019). Responses of reactive oxygen species and methylglyoxal metabolisms to magnesium-deficiency differ greatly among the roots, upper and lower leaves of *Citrus sinensis*. *BMC Plant Biol.* 19:76. doi: 10.1186/s12870-019-1683-4

Cakmak, I. (2005). The role of potassium in alleviating detrimental effects of abiotic stresses in plants. *J. Plant Nutr. Soil Sci.* 168, 521–530. doi: 10.1002/jpln.200420485

Cakmak, I., and Kirkby, E. A. (2008). Role of magnesium in carbon partitioning and alleviating photooxidative damage. *Physiol. Plant.* 133, 692–704. doi: 10.1111/j.1399-3054.2007.01042.x

Carstensen, A., Herdean, A., Birkelund Schmidt, S., Sharma, A., Spetea, C., Pribil, M., et al. (2018). The impacts of phosphorus deficiency on the photosynthetic electron transport chain. *Plant Physiol.* 177, 271–284. doi: 10.1104/pp.17.01624

Ceppi, M. G., Oukarroum, A., Çiçek, N., Strasser, R. J., and Schansker, G. (2012). The IP amplitude of the fluorescence rise OJIP is sensitive to changes in the photosystem I content of leaves: a study on plants exposed to magnesium and sulfate deficiencies, drought stress and salt stress. *Physiol. Plant.* 144, 277–288. doi: 10.1111/j.1399-3054.2011.01549.x

Cetner, M. D., Kalaji, H. M., Borucki, W., and Kowalczyk, K. (2020). Phosphorus deficiency affects the I-step of chlorophyll *a* fluorescence induction curve of radish. *Photosynthetica* 58, 671–681. doi: 10.32615/ps.2020.015

Çiçek, N., Oukarroum, A., Strasser, R. J., and Schansker, G. (2018). Salt stress effects on the photosynthetic electron transport chain in two chickpea lines differing in their salt stress tolerance. *Photosynth. Res.* 136, 291–301. doi: 10.1007/s11120-017-0463-y

De Freitas, S. T., Vidal, C., Do Amarante, T., and Mitcham, E. J. (2016). "Calcium disorders in plants," in *Postharvest Ripening Physiology of Crops*. ed. S. Pareek (Boca Raton: CRC Press).

Dell, B., and Huang, L. (1997). Physiological response of plants to low boron. *Plant Soil* 193, 103–120. doi: 10.1023/A:1004264009230

Delosme, R. (1967). Études de l'induction de fluorescence des algues vertes et des chloroplastes au début d'une illumination intense. *Biochim. Biophys. Acta* 143, 108–128. doi: 10.1016/0005-2728(67)90115-6

Dinç, E., Ceppi, M. G., Tóth, S. Z., Bottka, S., and Schansker, G. (2012). The chl *a* fluorescence intensity is remarkably insensitive to changes in the chlorophyll content of the leaf as long as the chl *a/b* ratio remains unaffected. *Biochim. Biophys. Acta* 1817, 770–779. doi: 10.1016/j.bbabio.2012.02.003

Evans, J. R., and Terashima, I. (1988). Photosynthetic characteristics of spinach leaves grown with different nitrogen treatments. *Plant Cell Physiol.* 29, 157–165. doi: 10.1093/oxfordjournals.pcp.a077462

Fischer, E. S., and Bremer, E. (1993). Influence of magnesium deficiency on rates of leaf expansion, starch and sucrose accumulation, and net assimilation in *Phaseolus vulgaris*. *Physiol. Plant.* 89, 271–276. doi: 10.1111/j.1399-3054.1993.tb00153.x

Frydenvang, J., Van Maarschalkerweerd, M., Carstensen, A., Mundus, S., Birkelund Schmidt, S., Rosager Pedas, P., et al. (2015). Sensitive detection of phosphorus deficiency in plants using chlorophyll *a* fluorescence. *Plant Physiol.* 169, 353–361. doi: 10.1104/pp.15.00823

Hajiboland, R., and Farhanghi, F. (2010). Remobilization of boron, photosynthesis, phenolic metabolism and anti-oxidant defense capacity in boron-deficient turnip (*Brassica rapa* L.) plants. *Soil Sci. Plant Nutr.* 56, 427–437. doi: 10.1111/j.1747-0765.2010.00478.x

Hall, J. D., Bar, R., Al-Abbas, A. H., and Crane, F. L. (1972). Ultrastructure of chloroplasts in mineral-deficient maize leaves. *Plant Physiol.* 50, 404–409. doi: 10.1104/pp.50.3.404

Han, S., Chen, L.-S., Jiang, H.-X., Smith, B. R., Yang, L.-T., and Xie, C.-Y. (2008). Boron deficiency decreases growth and photosynthesis, and increases starch and hexoses in leaves of citrus seedlings. *J. Plant Physiol.* 165, 1331–1341. doi: 10.1016/j.jplph.2007.11.002

Hauer-Jákli, M., and Tränkner, M. (2019). Critical leaf magnesium thresholds and the impact of magnesium on plant growth and photo-oxidative defense: A systemic review and meta-analysis from 70 years of research. *Front. Plant Sci.* 10:766. doi: 10.3389/fpls.2019.00766

Hermans, C., Bourgis, F., Faucher, M., Strasser, R. J., Delrot, S., and Verbruggen, N. (2005). Magnesium deficiency in sugar beets alters sugar partitioning and phloem loading in young mature leaves. *Planta* 220, 541–549. doi: 10.1007/s00425-004-1376-5

Husted, S., Laursen, K. H., Hebbern, C. A., Schmidt, S. B., Pedas, P., Haldrup, A., et al. (2009). Manganese deficiency leads to genotype-specific changes in fluorescence induction kinetics and state transitions. *Plant Physiol.* 150, 825–833. doi: 10.1104/pp.108.134601

Ide, Y., Kusano, M., Oikawa, A., Fukushima, A., Tomatsu, H., Saito, K., et al. (2011). Effects of molybdenum deficiency and defects in molybdate transporter MOT1 on transcript accumulation and nitrogen/sulphus metabolism in *Arabidopsis thaliana*. *J. Exp. Bot.* 62, 1483–1497. doi: 10.1093/jxb/erq345

Liakopoulos, G., Stavrianakou, S., Filippou, M., Fasseas, C., Tsadilas, C., Drossopoulos, I., et al. (2005). Boron remobilization at low boron supply in olive (*Olea europaea*) in relation to leaf and phloem mannitol concentrations. *Tree Physiol.* 25, 157–165. doi: 10.1093/treephys/25.2.157

Lu, Y.-B., Yang, L.-T., Li, Y., Xu, J., Liao, T.-T., Chen, Y.-B., et al. (2014). Effects of boron deficiency on major metabolites, key enzymes and gas exchange in leaves and roots of *Citrus sinensis* seedlings. *Tree Physiol.* 34, 608–618. doi: 10.1093/treephys/tpu047

Mahler, R. L. (1982). *Molybdenum in Idaho*. Idaho: University of Idaho.

Merchant, S. S., Allen, M. D., Kropat, J., Moseley, J. L., Long, J. C., Tottey, S., et al. (2006). Between a rock and a hard place: trace element nutrition in Chlamydomonas. *Biochim. Biophys. Acta* 1763, 578–594. doi: 10.1016/j.bbamcr.2006.04.007

Morin, P. (1964). Études des cinétiques de fluorescence de la chlorophylle in vivo, dans les premiers instants qui suivent le début de l'illumination. *J. Chim. Phys.* 61, 674–680. doi: 10.1051/jcp/1964610674

Nguyen, N. T., Nakabayashi, K., Mohapatra, P. K., Thompson, J., and Fujita, K. (2003). Effect of nitrogen deficiency on biomass production, photosynthesis, carbon partitioning and nitrogen nutrition status of *Melaleuca* and *Eucalyptus* species. *Soil Sci. Plant Nutr.* 49, 99–109. doi: 10.1080/00380768.2003.10409985

Ohnishi, M., Furutani, R., Sohtome, T., Suzuki, T., Wada, S., Tanaka, S., et al. (2021). Photosynthetic parameters show specific responses to essential mineral deficiencies. *Antioxidants* 10:996. doi: 10.3390/antiox10070996

Peng, Y. Y., Liao, L. L., Liu, S., Nie, M. M., Li, J., Zhang, L. D., et al. (2019). Magnesium deficiency triggers SGR-mediated chlorophyll degradation for magnesium remobilization. *Plant Physiol.* 181, 262–275. doi: 10.1104/pp.19.00610

Pfündel, E. E. (2021). Simultaneously measuring pulse-amplitude-modulated (PAM) chlorophyll fluorescence of leaves at wavelengths shorter and longer than 700 nm. *Photosynth. Res.* 147, 345–358. doi: 10.1007/s11120-021-00821-7

Ridolfi, M., Roupsard, O., Garrec, J. P., and Dreyer, E. (1996). Effects of a calcium deficiency on stomatal conductance and photosynthetic activity of *Quercus robur* seedlings grown on nutrient solution. *Ann. Sci. For.* 53, 325–335. doi: 10.1051/forest:19960215

Schansker, G., Tóth, S. Z., and Strasser, R. J. (2005). Methylviologen and dibromothymoquinone treatments of pea leaves reveal the role of photosystem I in the Chl *a* fluorescence rise OJIP. *Biochim. Biophys. Acta* 1706, 250–261. doi: 10.1016/j.bbabio.2004.11.006

Schansker, G., and Van Rensen, J. J. S. (1999). Performance of active photosystem II centers in photoinhibited pea leaves. *Photosynth. Res.* 62, 175–184. doi: 10.1023/A:1006374707722

Schmidt, S. B., Powikrowska, M., Krogholm, K. S., Naumann-Busch, B., Schjoerring, J. K., Husted, S., et al. (2016). Photosystem II functionality in barley responds dynamically to changes in leaf manganese status. *Front. Plant Sci.* 7:1772. doi: 10.3389/fpls.2016.01772

Schreiber, U., and Klughammer, C. (2021). Evidence for variable chlorophyll fluorescence of photosystem I in vivo. *Photosynth. Res.* 149, 213–231. doi: 10.1007/s11120-020-00814-y

Schreiber, U., Klughammer, C., and Schansker, G. (2019). Rapidly reversible chlorophyll fluorescence quenching induced by pulse of supersaturating light in vivo. *Photosynth. Res.* 142, 35–50. doi: 10.1007/s11120-019-00644-7

Shao, C.-H., Qiu, C.-F., Qian, Y.-F., and Liu, G.-R. (2020). Nitrate deficiency decreased photosynthesis and oxidation-reduction processes, but increased cellular transport, lignin biosynthesis and flavonoid metabolism revealed by RNA-seq in *Oryza sativa* leaves. *PLoS One* 15:e0235975. doi: 10.1371/journal.pone.0235975

Spiller, S., and Terry, N. (1980). Limiting factors in photosynthesis; II. Iron stress diminishes photochemical capacity by reducing the number of photosynthetic units. *Plant Physiol.* 65, 121–125. doi: 10.1104/pp.65.1.121

Srivastava, A., Guissé, B., Greppin, H., and Strasser, R. J. (1997). Regulation of antenna structure and electron transport in photosystem II of *Pisum sativum* under elevated temperature probed by the fast polyphasic chlorophyll a fluorescence transient: OKJIP. *Biochim. Biophys. Acta* 1320, 95–106. doi: 10.1016/S0005-2728(97)00017-0

Tainer, J. A., Getzoff, E. D., Richardson, J. S., and Richardson, D. C. (1983). Structure and mechanism of copper, zinc superoxide dismutase. *Nature* 306, 284–287. doi: 10.1038/306284a0

Terry, N., and Huston, R. P. (1975). Effects of calcium on the photosynthesis of intact leaves and isolated chloroplasts of sugar beets. *Plant Physiol.* 55, 923–927. doi: 10.1104/pp.55.5.923

Terry, N., and Ulrich, A. (1974). Effects of magnesium deficiency on the photosynthesis and respiration of leaves of sugar beet. *Plant Physiol.* 54, 379–381. doi: 10.1104/pp.54.3.379

Tóth, S. Z., Schansker, G., Garab, G., and Strasser, R. J. (2007a). Photosynthetic electron transport activity in heat-treated barley leaves: the role of internal alternative electron donors to photosystem II. *Biochim. Biophys. Acta* 1767, 295–305. doi: 10.1016/j.bbabio.2007.02.019

Tóth, S. Z., Schansker, G., Kissimon, J., Kovács, L., Garab, G., and Strasser, R. J. (2005). Biophysical studies of photosystem II-related recovery processes after a heat pulse in barley seedlings (*Hordeum vulgare* L.). *J. Plant Physiol.* 162, 181–194. doi: 10.1016/j.jplph.2004.06.010

Tóth, S. Z., Schansker, G., and Strasser, R. J. (2007b). A non-invasive assay of the plastoquinone pool redox state based on the OJIP-transient. *Photosynth. Res.* 93, 193–203. doi: 10.1007/s11120-007-9179-8

Van Wijk, K. J., and Krause, G. H. (1991). O$_2$-dependence of photoinhibition at low temperature in intact protoplasts of *Locusta valerianella* L. *Planta* 186, 135–142. doi: 10.1007/BF00201509

Yamasaki, H., Pilon, M., and Shikanai, T. (2008). How do plants respond to copper deficiency? *Plant Signal. Behav.* 3, 231–232. doi: 10.4161/psb.3.4.5094

Zivcak, M., Brestic, M., Kunderlikova, K., Olsovska, K., and Allakhverdiev, S. I. (2015). Effect of photosystem I inactivation on chlorophyll a fluorescence induction in wheat leaves: does activity of photosystem I play any role in OJIP rise? *J. Photochem. Photobiol.* 152, 318–324. doi: 10.1016/j.jphotobiol.2015.08.024